



doi:10.1016/j.gca.2003.08.020

Sources of osmium to the modern oceans: New evidence from the ^{190}Pt - ^{186}Os system

DIANE K. MCDANIEL,^{1,*} RICHARD J. WALKER,¹ SIDNEY R. HEMMING,² MARY F. HORAN,³ HARRY BECKER,¹ and RICHARD I. GRAUCH⁴¹Isotope Geochemistry Laboratory, Department of Geology, University of Maryland, College Park, MD 20742, USA²Department of Earth and Environmental Sciences, Lamont-Doherty Observatory of Columbia University, Rt. 9W, Palisades, NY 10964, USA³Department of Terrestrial Magnetism, Carnegie Institution of Washington, 5241 Broad Branch Road NW, Washington, DC 20015, USA⁴United States Geological Survey, Denver Federal Center, MS 973, Denver, CO 80225, USA

(Received March 7, 2003; accepted in revised form August 21, 2003)

Abstract—High precision Os isotope analysis of young marine manganese nodules indicate that whereas the composition of modern seawater is radiogenic with respect to $^{187}\text{Os}/^{188}\text{Os}$, it has $^{186}\text{Os}/^{188}\text{Os}$ that is within uncertainty of the chondritic value. Marine Mn nodule compositions thus indicate that the average continental source of Os to modern seawater had long-term high Re/Os compared to Pt/Os. Analyses of loess and freshwater Mn nodules support existing evidence that average upper continental crust (UCC) has resolvably suprachondritic $^{186}\text{Os}/^{188}\text{Os}$, as well as radiogenic $^{187}\text{Os}/^{188}\text{Os}$. Modeling the composition of seawater as a two-component mixture of oceanic/cosmic Os with chondritic Os compositions and continentally-derived Os demonstrates that, insofar as estimates for the composition of average UCC are accurate, congruently weathered average UCC cannot be the sole continental source of Os to seawater. Our analysis of four Cambrian black shales confirm that organic-rich sediments can have $^{187}\text{Os}/^{188}\text{Os}$ ratios that are much higher than average UCC, but $^{186}\text{Os}/^{188}\text{Os}$ compositions that are generally between those of chondrites and average-UCC. Preferential weathering of black shales can result in dissolved Os discharged to the ocean basins that has a much lower $^{186}\text{Os}/^{188}\text{Os}$ than does average upper crust. Modeling the available data demonstrates that augmentation of estimated average UCC compositions with less than 0.1% additional black shale and 1.4% additional ultramafic rock can produce a continental end-member Os isotopic composition that satisfies the requirements imposed by the marine Mn nodule data. The interplay of these two sources provides a mechanism by which the $^{187}\text{Os}/^{188}\text{Os}$ of seawater can change as sources and weathering conditions change, yet seawater $^{186}\text{Os}/^{188}\text{Os}$ varies only minimally. Copyright © 2004 Elsevier Ltd

1. INTRODUCTION

The ^{187}Re - ^{187}Os and ^{87}Rb - ^{87}Sr isotope systems have been used to help understand sources and rates of continental denudation during the Cenozoic, and to delineate changes in chemical weathering rates and the delivery of crustal Os and Sr to the world's oceans (e.g., Palmer and Edmond, 1989; Pegram et al., 1992; Raymo and Ruddiman, 1992; Ravizza, 1993; Peucker-Ehrenbrink et al., 1995). Erosion rates and the provenance and proportion of continental (and potentially oceanic) Os and Sr contributing to seawater have varied significantly over the past 65 Ma. Since this time, seawater $^{187}\text{Os}/^{188}\text{Os}$ and $^{87}\text{Sr}/^{86}\text{Sr}$ have increased gradually. This has been attributed by some to increased rates of uplift and denudation in the Alpine-Himalayan mountain belt and the American Cordillera, although the same trend can be produced by changes in the relative contributions of chemically dissimilar sources (e.g., Pegram et al., 1992; Raymo and Ruddiman, 1992; Ravizza, 1993; Peucker-Ehrenbrink et al., 1995; Blum et al., 1998; Derry and France-Lanord, 1996; Quade et al., 1997). The latter alternative may be most consistent with the observation that Os and Sr isotopic compositions appear to have been decoupled between ~60 and 40 Ma, when $^{87}\text{Sr}/^{86}\text{Sr}$ remained nearly constant but $^{187}\text{Os}/^{188}\text{Os}$ increased substantially, and between ~30 and 15 Ma, when $^{87}\text{Sr}/^{86}\text{Sr}$ increased rapidly, but $^{187}\text{Os}/^{188}\text{Os}$ remained nearly constant (Pegram et al., 1992; Ravizza, 1993; Peucker-

Ehrenbrink et al., 1995; Reusch et al., 1998; MacArthur et al., 2001).

The high $^{187}\text{Os}/^{188}\text{Os}$ and $^{87}\text{Sr}/^{86}\text{Sr}$ ratios for modern seawater (e.g., Burke et al., 1982; DePaolo, 1986; Sharma et al., 1997; Levasseur et al., 1998; Woodhouse et al., 1999), require that much of the Os and Sr present in modern seawater is derived from chemical weathering of radiogenic continental crust. For example, modern seawater has a $^{187}\text{Os}/^{188}\text{Os}$ of ~1.05 (Sharma et al., 1997; Levasseur et al., 1998; Woodhouse et al., 1999), whereas young oceanic crust and cosmic dust has generally chondritic $^{187}\text{Os}/^{188}\text{Os}$ of ~0.13 (Shirey and Walker, 1998). Estimates for the $^{187}\text{Os}/^{188}\text{Os}$ of continentally-derived Os range from 1.26 to 1.54 (e.g., Esser and Turekian, 1988; Esser and Turekian, 1993; Peucker-Ehrenbrink et al., 1995; Sharma and Wasserburg, 1997). On this basis, it has been estimated that from 70 to 80% of the Os present in modern seawater has a continental provenance, and the remaining 20 to 30% originates from hydrothermal interactions with young oceanic crust at ocean spreading centers, and from the influx and dissolution of cosmic dust (Sharma et al., 1997; Levasseur et al., 1999). The sources of continental Os and the transport mechanisms delivering it to the oceans are the subject of considerable research (e.g., Pegram et al., 1994; Peucker-Ehrenbrink and Ravizza, 1996; Levasseur et al., 1999; Sharma et al., 1999; Jaffe et al., 2002; Williams and Turekian, 2002).

Although typically quite radiogenic, $^{187}\text{Os}/^{188}\text{Os}$ ratios and Os abundances are extremely variable in continental rocks. Young mafic rocks with low Os abundances, and both young and ancient ultramafic rocks with high Os abundances (e.g., peridotites and komatiites), are characterized by generally un-

* Author to whom correspondence should be addressed. (dkmcd@comcast.net).

radiogenic $^{187}\text{Os}/^{188}\text{Os}$ (<0.2); felsic rocks, sediments, and ancient mafic rocks tend to have much more radiogenic $^{187}\text{Os}/^{188}\text{Os}$ (≥ 0.2), and quite variable Os abundances (Shirey and Walker, 1998; Walker et al., 2002; Williams and Turekian, 2002). Organic-rich black shales are notable sediments with regard to the mass balance of Os in the crust in that they can have very high abundances of Os and Re and very radiogenic $^{187}\text{Os}/^{188}\text{Os}$ (e.g., Ravizza and Esser, 1993; Horan et al., 1994; Cohen et al., 1999; Singh et al., 1999; Pierson-Wickmann et al., 2000; Ripley et al., 2001; Creaser et al., 2002). For developing global climate change models, it is especially important to constrain the proportion of silicates to organic-rich sediments weathered, given that silicate weathering ultimately consumes atmospheric CO_2 , whereas the weathering of organic rich sediments releases CO_2 .

Here, we investigate potential continental sources of Os to the oceans using the ^{187}Re - ^{187}Os system in tandem with the ^{190}Pt - ^{186}Os system. The coupled systems can provide unique insights to distinguish among possible continental crustal sources, given that they reflect both long-term Re/Os and Pt/Os ratios (Ravizza et al., 1998; Walker et al., 1999). The ^{190}Pt - ^{186}Os system ($^{190}\text{Pt} \rightarrow ^{186}\text{Os} + \alpha$) has received far less attention than the ^{187}Re - ^{187}Os system because ^{190}Pt is a minor Pt isotope (0.013 atomic %) with a small decay constant ($1.477 \times 10^{-12} \text{a}^{-1}$) (Walker et al., 1997; Morgan et al., 2002), leading to only minor production of ^{186}Os in most systems through geologic time. As with $^{187}\text{Os}/^{188}\text{Os}$ and Re/Os, the $^{186}\text{Os}/^{188}\text{Os}$ and long-term Pt/Os of the upper mantle are generally chondritic ($^{186}\text{Os}/^{188}\text{Os} = 0.119834 \pm 2$, Pt/Os ≈ 2) (Walker et al., 1997; Brandon et al., 2000). Key to the coupled application of the ^{187}Re - ^{187}Os and ^{190}Pt - ^{186}Os systems however, is the observation that some continental lithologies with very high Re/Os have quite low Pt/Os (e.g., Horan et al., 1994; Peucker-Ehrenbrink and Jahn, 2001).

2. SAMPLES AND ANALYTICAL METHODS

Samples were collected and analyzed to further two related goals: to characterize the $^{186}\text{Os}/^{188}\text{Os}$ composition of recent seawater, and to characterize the coupled $^{186}\text{Os}/^{188}\text{Os}$ and $^{187}\text{Os}/^{188}\text{Os}$ compositions of potential continental sources of Os to seawater. To obtain high-precision $^{186}\text{Os}/^{188}\text{Os}$ measurements, 30–40 ng of Os were needed for each mass spectrometric analysis. Sample selections and sizes thus take into account the amount of Os needed for a successful analysis. Because it has very low Os abundances (on the order of only 10's of parts per trillion), direct analysis of typical upper crustal material is particularly difficult, and requires processing a kg or more of material for a successful high-precision $^{186}\text{Os}/^{188}\text{Os}$ analysis.

The Os isotopic composition of Cenozoic seawater is determined here using marine Mn nodules as proxies for seawater. Marine Mn nodules generally record the Os isotopic compositions of the seawater from which they precipitate (Luck and Turekian, 1983; Palmer et al., 1988). Because of the moderate sample sizes required for $^{186}\text{Os}/^{188}\text{Os}$ analysis, and slow growth rates of Mn nodules (typically 0.5–2 mm/Ma; Lyle, 1982), the Os isotopic compositions of an aliquant of rock integrate seawater Os compositions over relatively large time increments (as much as several million years). Accordingly, the

$^{186}\text{Os}/^{188}\text{Os}$ compositions of Mn nodules cannot be used for detailed chemostratigraphic analysis of the marine record. Nonetheless, they are preferable to rapidly deposited pelagic sediment because of their high Os abundances (Luck and Turekian, 1983; Palmer and Turekian, 1986; Burton et al., 1999). Other samples analyzed include Pleistocene loess, a lacustrine Mn crust, and several organic-rich black shales. The loess was collected from a quickly eroding outcrop on the campus of SUNY Stony Brook, Long Island, NY; two 1.2 kg samples were collected approximately 1 yr apart. These samples provide information on the average bulk isotopic composition of the upper continental crust (UCC). A 1 kg sample of a freshwater Mn crust from Lake Oneida, NY, was analyzed to provide a measure of continental Os released into the hydrosphere. We also analyzed four Cambrian sulfide-rich black shales from the Hunan Province, China, to characterize the ^{186}Os - ^{187}Os systematics of organic-rich sediments. The high Os abundances in these samples allowed us to analyze aliquants of only approximately 1 g.

For all samples but the black shales, a Ni sulfide fire assay technique was used to preconcentrate the Os (Hoffman et al., 1978; Brandon et al., 1999). Samples for isotopic composition analysis were not spiked for isotope dilution because of possible effects from the uncertainty of the spike correction on $^{186}\text{Os}/^{188}\text{Os}$. Platinum, Re and Os abundances of the Mn nodules and loess were analyzed by isotope dilution on separate powder aliquants. The concentrations of these elements in the black shales were originally reported by Horan et al. (1994). All samples (including the black shales) were then processed using Carius tube digestion and solvent extraction techniques (Walker et al., 1997; Brandon et al., 1999). Osmium isotopes were analyzed by negative thermal ionization mass spectrometry using a Sector 54 mass spectrometer at the University of Maryland. Total procedural yields for Os were 75–90%. Blanks were approximately 0.7 pg per gram of sample fused and have $^{186}\text{Os}/^{188}\text{Os} = 0.1199 \pm 2$ and $^{187}\text{Os}/^{188}\text{Os} = 0.125 \pm 5$ (2σ). This corresponds to a 'worst-case' sample/blank ratio of 30:1 for the lowest abundance samples, and more commonly, of 1500:1 for samples with 1 ppb Os.

Two data acquisition routines were used to collect the data. Marine Mn nodules were run using a multi-dynamic solution, wherein nine analyses of a Johnson-Matthey standard solution yielded $^{186}\text{Os}/^{188}\text{Os} = 0.1198441 \pm 36$ and $^{187}\text{Os}/^{188}\text{Os} = 0.113763 \pm 33$ ($2\sigma_{\text{pop}}$). We subsequently modified the data collection to a static routine, permitting more accurate monitoring of the high-mass baseline for mass 234 ($^{186}\text{Os}^{16}\text{O}_3^-$). This was crucial for samples with very high $^{187}\text{Os}/^{188}\text{Os}$ (black shales), as the tail from the very strong mass-235 ($^{187}\text{Os}^{16}\text{O}_3^-$) peak tended to extend to mass 234. Our first attempt to overcome this obstacle was by using the Sector 54 software's baseline correction routine, inputting a tailing factor that we determined manually by using an electron multiplier and graphing software. We determined that this method overcorrected standard runs, and therefore did not use it for samples. For the runs reported here, we resorted to monitoring the baseline position with the electron multiplier before and after the routine. Analyses were considered acceptable if counts at the high half-mass (234.5) were sufficiently low to avoid effects on the $^{186}\text{Os}/^{188}\text{Os}$ in the sixth significant digit. This method had two consequences: 1) we were not able to analyze samples with

Table 1. $^{186}\text{Os}/^{188}\text{Os}$ and $^{187}\text{Os}/^{188}\text{Os}$ compositions of marine and crustal samples analyzed in this study.^a

Sample	Location	$^{186}\text{Os}/^{188}\text{Os}$	$^{187}\text{Os}/^{188}\text{Os}$	Re (ppb)	Pt (ppb)	Os (ppb)	$^{187}\text{Re}/^{188}\text{Os}$	$^{190}\text{Pt}/^{188}\text{Os}$
Mn nodules								
VM19-D11	A	New England Sea Mounts	0.119827 (9)	0.95181 (3)	0.152	0.8379	0.968	
	A		0.119820 (14)	0.94141 (4)				
	B		0.119835 (16)	0.94572 (4)				
	C		0.119834 (8)	0.94065 (2)				
	D		0.119831 (12)	0.95152 (4)				
	mean		0.119829 (11)	0.946 (10)				
VM15-SBT151	A	Puerto Rico Trench	0.119829 (6)	0.95672 (2)	0.026	166	3.15	0.038
	B		0.119847 (6)	0.96722 (2)				
VM15-SBT125		S. Labrador Sea	0.119818 (15)	1.02918 (4)	0.0531	52.8	0.6290	0.454
VM34-RD6		east of New Guinea	0.119836 (16)	0.63976 (5)	0.027	686	0.6342	0.213
VM21-D5	A	north central Pacific	0.119827 (34)	0.97279 (7)	0.0243		0.6735	0.193
	B		0.119870 (10)	0.85009 (3)				
	B		0.119843 (15)	0.82907 (4)				
VM34-D25		Agulhas Plateau	0.119825 (13)	1.01051 (4)	0.01727	146	0.4785	0.194
RC14-D4		Mozambique channel	0.119815 (20)	0.86602 (5)				0.33
Crustal samples								
LIL	A	Long Island loess	0.119866 (16)	0.74613 (3)	0.08	0.4	0.022	20.2
	B		0.119849 (10)	0.66998 (2)				
LOMN		Lake Oneida Mn nodule	0.119856 (7)	1.91606 (3)	5.6	1.5	0.112	296
Black shales DP 4A14		Daping, China	0.119850 (26)	8.18302 (38)	15030*	690*	176.7*	841
			0.119840 (12)	8.19922 (21)				
			0.119853 (9)	8.18478 (15)				
			0.119847 (9)	8.18439 (15)				
			mean	0.119848 (10)				
SC 1A		Sansha, China	0.119842 (36)	9.7941 (8)	6720*	91*	65.9*	1111
GZP 5I		Ganziping, China	0.119841 (10)	7.82492 (14)	5550*	250*	65.6*	817
GZP 4E		Ganziping, China	0.119832 (14)	11.6144 (4)	10280*	190*	108.9*	1136
			0.119853 (36)	11.5699 (9)				

^a Letters after sample names (A–D) identify subsamples either different portions of the same Mn nodule or separate field samples. Errors in parentheses are the in-run $2\sigma_m$ and refer to the last digit(s) of the results. Errors are similar to or larger than the external reproducibility of standard runs. Errors are better than 0.5% for Os and Re, and better than 10% for Pt. Errors for the mean of multiple analyses are $2\sigma_{pop}$.

* Re, Pt, Os abundances for black shales from Horan et al. (1994)

$^{187}\text{Os}/^{188}\text{Os}$ greater than 12, and 2) maintaining low baselines often required run conditions with lower oxygen pressure than is normally used. Oxygen is normally bled into the source region to facilitate the generation of the Os oxides measured. The reduction in oxygen pressure tended to decrease signal intensity. This second consequence is evident in data for black shales that is somewhat less precise than for other samples with much lower Os abundances. Since the static routine was faster than the multi-dynamic routine, it was also used for subsequent analyses of the loess and lacustrine Mn crust. Using the static routine, 13 analyses of a Johnson-Matthey standard yielded $^{186}\text{Os}/^{188}\text{Os} = 0.1198449 \pm 42$ and $^{187}\text{Os}/^{188}\text{Os} = 0.113846 \pm 39$ ($2\sigma_{pop}$).

As a reference, we use the chondrite $^{186}\text{Os}/^{188}\text{Os}$ value of 0.119834 ± 2 determined by Walker et al. (1997), and have corrected our data to the standard values reported therein ($^{186}\text{Os}/^{188}\text{Os} = 0.1198480 \pm 62$ and $^{187}\text{Os}/^{188}\text{Os} = 0.113791 \pm 9$, $n = 12$) for consistency. Isotope dilution measurements for Os and Re were made on an NBS 12^{cc} single-collector mass spectrometer in negative ion mode at the University of Maryland. Isotope dilution measurements for Pt were made using the Plasma 54 multicollector ICP-MS facility at the Department of Terrestrial Magnetism, Carnegie Institution of Washington (marine Mn nodules), and the Nu Plasma multicollector

ICP-MS at the University of Maryland (loess and the freshwater Mn nodule).

3. RESULTS AND INTERPRETATION

3.1. Marine Mn Nodules and the Composition of Seawater

Analytical results for seven marine Mn nodules are reported in Table 1. Concentrations of Os and Re for the suite range from 0.48 to 3.15 ppb and 0.017 to 0.152 ppb, respectively. No age corrections have been applied to either $^{187}\text{Os}/^{188}\text{Os}$ or $^{186}\text{Os}/^{188}\text{Os}$ ratios, as postdepositional ingrowth of either isotope would be negligible for the likely ages of these samples. Of the seven Mn nodules analyzed, five have at least one aliquant with $^{187}\text{Os}/^{188}\text{Os} > 0.94$, sufficiently high that they must have integrated ages of 5 Ma or younger, based on seawater evolution curves (e.g., Ravizza, 1993; Peucker-Ehrenbrink et al., 1995). Accordingly, the $^{186}\text{Os}/^{188}\text{Os}$ of these samples are probably the most representative of recent seawater. The $^{186}\text{Os}/^{188}\text{Os}$ for both analyses of sample VM34-D25, both analyses of VM15-SBT125, and the aliquant of sample VM21-D5 with $^{187}\text{Os}/^{188}\text{Os} > 0.94$ are all within analytical uncertainty of chondritic. Samples VM34-RD6 and RC14-D4 are possibly older, with $^{187}\text{Os}/^{188}\text{Os}$ ratios of 0.640 and 0.866,

respectively, yet they also have $^{186}\text{Os}/^{188}\text{Os}$ within the range of chondrites. Replicates for most samples were prepared from different portions of the same nodule. The observed heterogeneity in $^{187}\text{Os}/^{188}\text{Os}$ of the nodule subsamples, therefore, is likely the result of the variable accumulation of Os over several hundreds of thousands to millions of years while the $^{187}\text{Os}/^{188}\text{Os}$ of seawater was changing. There is also some evidence that the $^{186}\text{Os}/^{188}\text{Os}$ of seawater may have been higher in the past. In particular, one precise analysis of nodule VM21-D5 is suprachondritic, with $^{186}\text{Os}/^{188}\text{Os}$ of 0.119870. We briefly discuss this below, but a detailed interpretation is premature in light of the limited data.

In previous studies of ^{186}Os variations in volcanic rocks, the data from multiple aliquants of sample powders were combined to reduce analytical uncertainties (Walker et al., 1997; Brandon et al., 1999). Of five aliquants of Mn nodule VM19-D11 (representing three nodule subsamples), all have $^{186}\text{Os}/^{188}\text{Os}$ within analytical uncertainties of one another (Fig. 1, inset). The $^{187}\text{Os}/^{188}\text{Os}$ of the five are more variable and range from 0.9407 to 0.9518. The $^{187}\text{Os}/^{188}\text{Os}$ ratios, again, indicate an integrated age younger than 5 Ma. The average $^{186}\text{Os}/^{188}\text{Os}$ of 0.119829 \pm 11 ($2\sigma_{\text{pop}}$) for the composite provides the tightest constraint on the $^{186}\text{Os}/^{188}\text{Os}$ of recent seawater, and is in good agreement with the chondritic ratio. If these samples are collectively representative of seawater during the past few million years, modern seawater must have a $^{186}\text{Os}/^{188}\text{Os}$ that is analytically indistinguishable from that of chondrites and the upper mantle (Fig. 1). Consequently, the highly radiogenic $^{187}\text{Os}/^{188}\text{Os}$, but chondritic $^{186}\text{Os}/^{188}\text{Os}$ ratios in these marine precipitates require sources that are characterized by relatively long-term high Re/Os and low Pt/Os.

3.2. $^{186}\text{Os}/^{188}\text{Os}$ of Continental Crust, Estimates, and Measurements

To delimit the $^{186}\text{Os}/^{188}\text{Os}$ ratio of potential continental crustal end-member sources of Os to seawater, it is necessary to know what their Pt, Os and $^{186}\text{Os}/^{188}\text{Os}$ compositions are. Although $^{187}\text{Os}/^{188}\text{Os}$ and Re, Pt, and Os abundances for average UCC are reported in the literature (e.g., Esser and Turekian, 1993; Wedepohl, 1995; Gao et al., 1998; Peucker-Ehrenbrink and Jahn, 2001), before this report there have been no direct $^{186}\text{Os}/^{188}\text{Os}$ measurements of representative modern upper crustal material. Besides direct measurement, published Pt/Os estimates of average UCC allow the prediction of expected $^{186}\text{Os}/^{188}\text{Os}$. Reported Pt/Os ratios for average UCC range from 8 (0.4 ppb Pt and 0.05 ppb Os; Wedepohl, 1995) to as high as 30 (1.5 ppb Pt and 0.050 ppb Os; Gao et al., 1998). Mafic rocks also typically have Pt/Os > 10 (Ravizza and Pyle, 1997), as does loess (Peucker Ehrenbrink and Jahn, 2001). Data for ores from the Sudbury Igneous Complex, generated as a result of bolide-induced crustal fusion, also provide support for a high Pt/Os for average UCC (Walker et al., 1991; Morgan et al., 2002). Over time, high Pt/Os must lead to an increase in $^{186}\text{Os}/^{188}\text{Os}$ that can be resolved from chondritic evolution (Pt/Os \cong 2). Assuming a chondritic starting composition, an average crustal residence age of 2.0 Ga (based on Nd model ages for average UCC, Miller et al., 1986) and Pt/Os \geq 8, average UCC should have a $^{186}\text{Os}/^{188}\text{Os}$ greater than 0.119850. Using similar calculations for Pt and Os data in loess, Peucker-

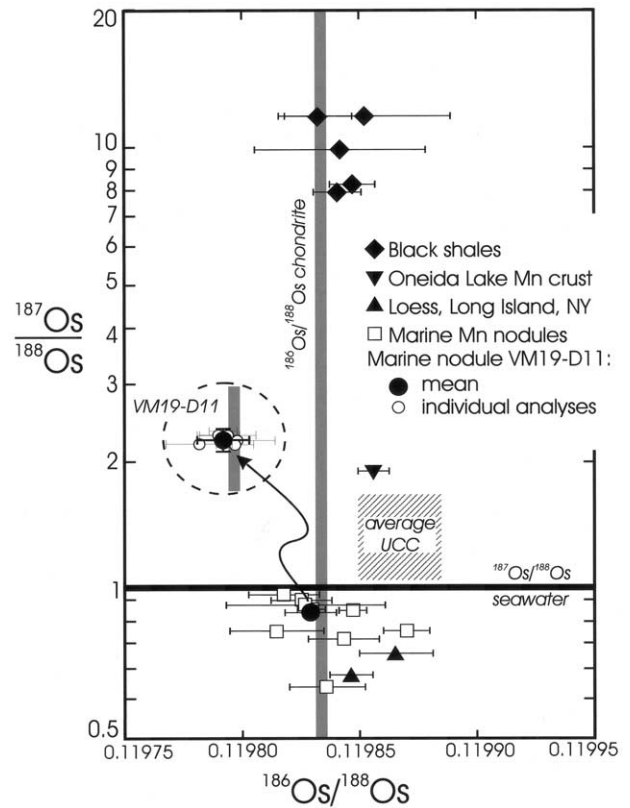


Fig. 1. Plot of $^{187}\text{Os}/^{188}\text{Os}$ (log scale) versus $^{186}\text{Os}/^{188}\text{Os}$ for marine Mn nodules, loess, a freshwater Mn crust, and black shales. Error bars are 2σ mean ($2\sigma_{\text{pop}}$ for the VM19-D11 composite). Most nodules with $^{187}\text{Os}/^{188}\text{Os}$ similar to that of modern seawater (horizontal black line) have $^{186}\text{Os}/^{188}\text{Os}$ that are consistent with the chondritic upper mantle (vertical gray line). Five analyses of a single Mn nodule, VM19-D11, have $^{186}\text{Os}/^{188}\text{Os}$ within error of each other and give a precise estimate of seawater $^{186}\text{Os}/^{188}\text{Os}$ that is within error of chondritic (inset, not magnified). Analyses for loess and freshwater Mn crust are suprachondritic, supporting a suprachondritic composition for average UCC (shaded box).

Ehrenbrink and Jahn (2001) estimated that average UCC has $^{186}\text{Os}/^{188}\text{Os} = 0.119885$. This range of estimates is plotted as a boxed field in Figure 1, using the $^{187}\text{Os}/^{188}\text{Os}$ estimate of Peucker-Ehrenbrink and Jahn (2001) for average UCC.

The two loess samples from Long Island, New York likely preferentially sampled Paleozoic Appalachian rocks from the north, and Nd model ages for them (T_{DM}) of 1.66 (LIL-A) and 1.60 (LIL-B) Ga (McDaniel, unpublished data) are somewhat younger than average UCC. Their $^{186}\text{Os}/^{188}\text{Os}$ ratios of 0.119866 \pm 16 and 0.119849 \pm 10 (2σ) (Table 1, Fig. 1), are enriched by a minimum of 140 and 30 ppm, respectively, over the chondritic ratio. Their $^{187}\text{Os}/^{188}\text{Os}$ ratios (0.75 and 0.67, respectively) are less radiogenic than seawater or average UCC, reflecting either a younger crustal residence time for the Os, derivation from low Re/Os terranes, or both. If these results are normalized to an age of 2 Ga and a Pt/Os \geq 8, the loess analyzed here suggest that average UCC has a minimum $^{186}\text{Os}/^{188}\text{Os}$ of 0.119855–0.119870.

A freshwater Mn crust from Oneida Lake, NY characterizes the average isotopic composition of Os weathered from the

catchment basin of the lake. Oneida Lake, with a small watershed of approximately 3500 km², is located on the North American craton in the Appalachian foreland. Feeder rivers sample Ordovician to Devonian quartzofeldspathic and carbonate sedimentary rocks, including shales. The ϵ_{Nd} of the analyzed Mn crust is -10.3 (McDaniel, unpublished data). The $^{147}\text{Sm}/^{144}\text{Nd}$ of the sample is noncrustal (0.137), indicating that Sm and Nd were likely fractionated during weathering and deposition. Assuming that the source of the Nd had a crustal $^{147}\text{Sm}/^{144}\text{Nd}$ (approximately 0.11) allows the estimation of 1.4 Ga for a T_{DM} . This sample has a $^{187}\text{Os}/^{188}\text{Os}$ of 1.916, comparable to analyses of Lake Oneida Mn crusts reported by Pegram et al. (1994) (~ 1.9), who concluded that the radiogenic $^{187}\text{Os}/^{188}\text{Os}$ was likely related to preferential weathering of black shales in the source area. The $^{186}\text{Os}/^{188}\text{Os}$ of 0.119856 ± 7 (2σ) is enriched by a minimum of 130 ppm over the chondritic value, indicating that the composition of Os released to the hydrosphere in this part of the Appalachian foreland is suprachondritic with respect to $^{186}\text{Os}/^{188}\text{Os}$. Again, renormalization to 2 Ga using $\text{Pt}/\text{Os} \geq 8$ suggests a minimum $^{186}\text{Os}/^{188}\text{Os}$ of approximately 0.119865.

By averaging the data for the loess and Mn crust, and using constraints on Pt/Os available from the literature, we tentatively conclude that the minimum $^{186}\text{Os}/^{188}\text{Os}$ likely for average UCC is 0.119850, with the expectation that it is probably considerably more radiogenic, and closer to the value of 0.119885 proposed by Peucker-Ehrenbrink and Jahn (2001).

3.3. $^{186}\text{Os}/^{188}\text{Os}$ of Black Shales

Organic-rich black shales, with much higher average Os contents and lower average Pt/Os than average UCC have been proposed as important sources of Os (and C) in modern seawater (Ravizza and Esser, 1993; Ravizza et al., 1998; Peucker-Ehrenbrink and Hannigan, 2000). Reduced sediment samples from the continental margins of Oman and west Africa have average Pt/Os ratios of only 5.3 (Ravizza and Pyle, 1997), and Pt/Os ratios ranging from approximately 1 to 4 have been reported for Paleozoic black shales from Canada and China (Horan et al., 1994). Organic-rich sediments are also characterized by very high Re/Os ratios and consequently, they rapidly evolve to highly radiogenic $^{187}\text{Os}/^{188}\text{Os}$ ratios (e.g., Ravizza and Esser, 1993; Horan et al., 1994; Pegram et al., 1994; Cohen et al., 1999; Singh et al., 1999; Pierson-Wickmann et al., 2000; Ripley et al., 2001; Creaser et al., 2002), but in general, in-situ growth of ^{186}Os should be much less than for average UCC. The $^{186}\text{Os}/^{188}\text{Os}$ of shale will depend not only on its Pt/Os since deposition, but also on the isotopic composition of Os incorporated during deposition, and thus may inherit Os with suprachondritic $^{186}\text{Os}/^{188}\text{Os}$. The Oneida Lake Mn crust described above may show evidence for this with a radiogenic $^{186}\text{Os}/^{188}\text{Os}$ that might have been inherited from black shales in the surrounding source area. Alternatively, the composition of the Mn crust composition may simply lie on a mixing line between black shales with chondritic $^{186}\text{Os}/^{188}\text{Os}$ and average UCC.

We analyzed four Cambrian sulfide-rich black shales from the Hunan Province of southern China with Re abundances of 5550 to 15,030 ppb, and $^{187}\text{Re}/^{188}\text{Os}$ ratios of over 800 (Horan

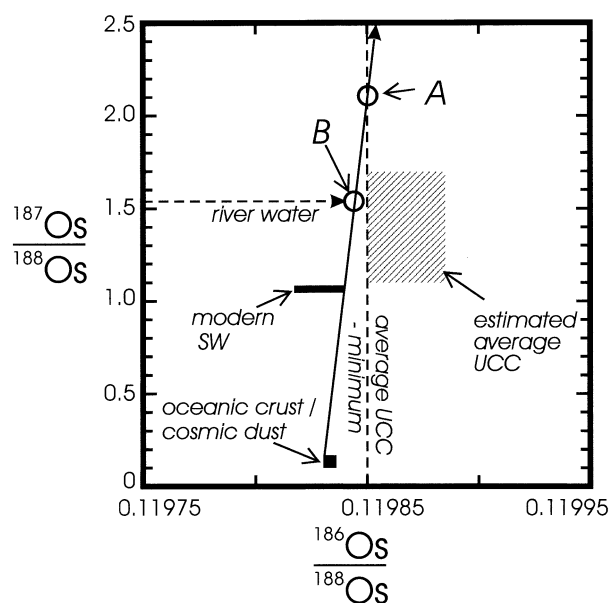


Fig. 2. Modeling the composition of seawater as a two-component mixture of oceanic/cosmic sources with a continentally derived end member places constraints on the average continental sources of Os to seawater. Black labeled box indicates our best estimate for modern seawater, calculated from the $^{186}\text{Os}/^{188}\text{Os}$ of the VM19-D11 composite and published seawater $^{187}\text{Os}/^{188}\text{Os}$. A mixing line (solid arrow) drawn from low estimates of chondritic oceanic/cosmic sources (labeled box) through the high $^{186}\text{Os}/^{188}\text{Os}$ limit of the seawater estimate projects to possible end-member compositions for the average continental source of Os to seawater. This continental end member must have an isotopic composition that falls on or to the left of this mixing line. Dashed vertical line projects the lower limit of average UCC estimates (ruled field) for $^{186}\text{Os}/^{188}\text{Os}$. Its intersection with the mixing line (point 'A') defines a minimum $^{187}\text{Os}/^{188}\text{Os} = 2.1$ for a continental end-member with $^{186}\text{Os}/^{188}\text{Os}$ characteristic of estimated average UCC. The dashed horizontal arrow projects an estimated average riverine $^{187}\text{Os}/^{188}\text{Os} = 1.54$, constraining the $^{186}\text{Os}/^{188}\text{Os}$ of a continental end member with this composition to 0.119844 or less. References for ocean crust, average UCC, seawater, and riverine compositions are in the text.

et al., 1994). The $^{187}\text{Os}/^{188}\text{Os}$ ratios for these shales are therefore quite high, varying from 7.82 to 11.6 (Fig. 1). Despite this, the $^{186}\text{Os}/^{188}\text{Os}$ ratios are unremarkable, in most cases within error of chondritic, and in no cases more radiogenic than low estimates of the average UCC.

4. DISCUSSION

The new, coupled ^{186}Os - ^{187}Os data allow constraints to be placed on the isotopic composition of Os being discharged from the continents into the world's oceans. These are illustrated on a plot of $^{187}\text{Os}/^{188}\text{Os}$ versus $^{186}\text{Os}/^{188}\text{Os}$, where the compositions of relevant reservoirs are shown (Fig. 2). If the Mn nodule $^{186}\text{Os}/^{188}\text{Os}$ analyses presented here are representative of modern seawater, then seawater has a generally chondritic $^{186}\text{Os}/^{188}\text{Os}$, coupled with a relatively radiogenic $^{187}\text{Os}/^{188}\text{Os}$. This inferred composition of seawater is plotted in a labeled box (Fig. 2) derived from the $^{186}\text{Os}/^{188}\text{Os}$ ratio of VM19-D11 (and its associated uncertainty), and the average $^{187}\text{Os}/^{188}\text{Os}$ of seawater reported by Sharma et al. (1997), Levasseur et al. (1998) and Woodhouse et al. (1999).

If Os in seawater is considered as a mixture of two source components, one oceanic and the other continentally derived, then the composition of seawater must lie along a straight mixing line between these two sources on a plot of $^{187}\text{Os}/^{188}\text{Os}$ versus $^{186}\text{Os}/^{188}\text{Os}$. The oceanic end member, which is also representative of cosmic dust sources, is chondritic with respect to both $^{186}\text{Os}/^{188}\text{Os}$ and $^{187}\text{Os}/^{188}\text{Os}$ (Shirey and Walker, 1998; Fig. 2). The continental source is the sum total of all dissolved Os that is discharged from the continents and continental margins into the ocean basins. This component is not necessarily identical in composition to average UCC. Projecting a mixing line from the minimum $^{186}\text{Os}/^{188}\text{Os}$ of the oceanic end member through the maximum $^{186}\text{Os}/^{188}\text{Os}$ of our seawater estimate (solid arrow, Fig. 2) defines a boundary such that the isotopic composition of the continental end member must lie on or to the left of that mixing line with a greater $^{187}\text{Os}/^{188}\text{Os}$ than modern seawater.

The hatched field that encompasses estimates of average UCC is to the right of the boundary mixing line, precluding it from representing the continental end member of seawater Os (Fig. 2). As in Figure 1, the range in $^{187}\text{Os}/^{188}\text{Os}$ for average UCC is derived from loess data and reported in Peucker Ehrenbrink and Jahn (2001). The range in $^{186}\text{Os}/^{188}\text{Os}$ for average UCC was discussed in section 3.2. That estimates for average UCC are not permissible as the continental end member may indicate that estimates for the $^{187}\text{Os}/^{188}\text{Os}$ of average UCC are not accurate. Although loess is among the best proxies available for average UCC, it may preferentially sample some types of continental crust over others (for instance, continental interiors). Projecting the mixing line to the minimum $^{186}\text{Os}/^{188}\text{Os}$ estimated for average UCC ($^{186}\text{Os}/^{188}\text{Os} \geq 0.119850$, vertical dashed line, Fig. 2) indicates that, for this scenario, average UCC must have a $^{187}\text{Os}/^{188}\text{Os}$ of 2.1 or greater (point A, Fig. 2) in order for it to be permissible as the continental end member for seawater Os. Higher $^{186}\text{Os}/^{188}\text{Os}$ for average UCC or lower $^{186}\text{Os}/^{188}\text{Os}$ for seawater require much higher $^{187}\text{Os}/^{188}\text{Os}$ (e.g., using $^{186}\text{Os}/^{188}\text{Os} = 0.11987$ requires a $^{187}\text{Os}/^{188}\text{Os}$ for average UCC of 4.5 or greater). $^{187}\text{Os}/^{188}\text{Os}$ ratios of this magnitude are significantly greater than current estimates for average UCC (Esser and Turekian, 1993; Peucker Ehrenbrink and Jahn, 2001). We consider it unlikely that these estimates of average UCC are so inaccurate.

An alternative and more easily accomplished explanation is that ^{187}Os – ^{186}Os constraints on average UCC are accurate, but average UCC may not be representative of the continental source of Os to seawater. In this case, the composition of seawater is not produced via representative sampling of average UCC, dissolving the Os within it quantitatively, and transferring this into the ocean basins. Rather, compositionally diverse parts of UCC may be sampled differentially during weathering and chemical denudation, and are thus variably represented in the Os that is finally discharged into the world's oceans. If chemical erosion preferentially samples one lithology over others, then the dissolved products will have a composition that falls somewhere between the preferred lithology and the others. Similarly, changes in climate, sea level, and topographic relief can tip the balance of erosion rates between craton interiors, continental margins, and modern island-arcs—all environments with distinct compositional suites of rocks. Of the elements typically used for tracing sources, Os is likely to

be particularly sensitive to preferential sampling, with an extreme range among different lithologies in the surface environment, both in terms of $^{187}\text{Os}/^{188}\text{Os}$ and in concentrations (over three orders of magnitude).

4.1. The Effects of Preferential Sampling of UCC

The two possible explanations for why estimates of average UCC cannot represent the continental end member for seawater Os—that estimates for average UCC are inaccurate, or that average UCC is not the sole source—are not mutually exclusive. Of the two options, however, we deem the second is likely to have the greater effect. Although loess may not representatively sample average UCC, for chemically labile elements, it is fundamental that dissolving UCC, a process in which chemical weathering predominates, will not. Two of the more important reservoirs of Os in UCC are black shales and ultramafic rocks (e.g., peridotites/serpentinites). Both types of rocks have high abundances of Os (Horan et al., 1994; Shirey and Walker, 1998; Cohen et al., 1999; Singh et al., 1999; Pierson-Wickmann et al., 2000; Creaser et al., 2002), and are also among the most easily weathered rock types, contributing high cation sums to rivers that drain them (Meybeck, 1987). Osmium is also more easily liberated from black shales during weathering than are most other elements, as it tends to be hosted by labile organic matter (Singh et al., 1999; Peucker-Ehrenbrink and Hannigan, 2000).

The continental end member for seawater Os can be modeled as the product of weathering a mixture of average UCC, black shales and ultramafic rocks (Fig. 3), allowing consideration of potential sensitivities of Os to mass balance. Although black shales and ultramafic rocks are represented within the construct of average UCC, they can also be treated as additional components to examine their potential impact on the Os budget during enhanced weathering and erosion. Average UCC is modeled assuming 0.03 ppb Os with a $^{187}\text{Os}/^{188}\text{Os}$ of 1.4 (Peucker-Ehrenbrink and Jahn, 2001), and a $^{186}\text{Os}/^{188}\text{Os}$ of 0.119880 (Fig. 3). Choosing a $^{186}\text{Os}/^{188}\text{Os}$ at the radiogenic end of available estimates provides a more rigorous test for the ability of the other two components to influence the mixture. An average concentration of 3 ppb Os, with chondritic $^{187}\text{Os}/^{188}\text{Os}$ and $^{186}\text{Os}/^{188}\text{Os}$, is assumed for ultramafic rocks (Shirey and Walker, 1998). Young mafic rocks also have isotopic compositions that fall at or near this end-member composition, although with much lower Os abundances, they do not have as pronounced an effect on a per mass basis as ultramafic rocks. Substantial increases in input from rivers eroding basalts in modern island-arc settings would have an effect that is similar to the addition of Os from ultramafic rocks.

The Os abundances and isotopic compositions of black shales are highly variable and an 'average' value is difficult to define. Black shale data from the literature, however, suggest that Os abundances from 0.1 to 5 ppb and $^{187}\text{Os}/^{188}\text{Os}$ from 1 to 10 or greater are common (Horan et al., 1994; Cohen et al., 1999; Singh et al., 1999; Pierson-Wickmann et al., 2000; Ripley et al., 2001; Creaser et al., 2002). Here, a $^{187}\text{Os}/^{188}\text{Os}$ of 9.3 and a $^{186}\text{Os}/^{188}\text{Os}$ of 0.119843 (the averages of our black shale data) are used in mixing calculations (Fig. 3). Osmium abundances are far higher in the samples we analyzed than is the norm, thus, a more typical Os abundance of 2 ppb is used to

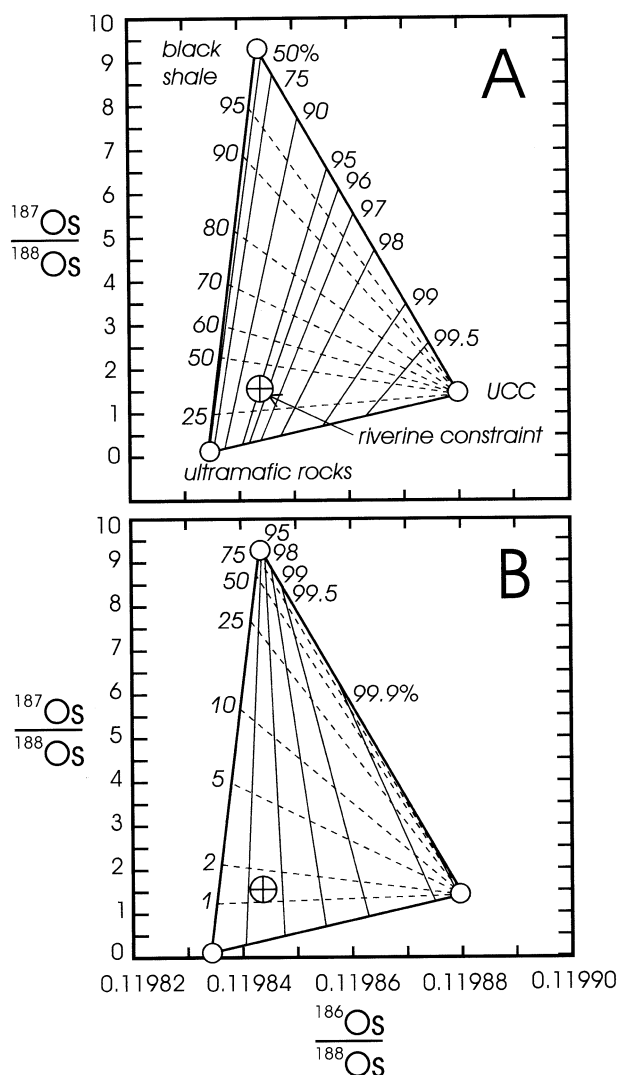


Fig. 3. Model calculations of the Os isotopic composition of average UCC that has been augmented by additional organic-rich black shales and ultramafic crust, illustrating the effects of preferential sampling of these continental lithologies during weathering. The choice of starting compositions are as follows (rationale and sources in text): average UCC, 0.03 ppb Os, $^{187}\text{Os}/^{188}\text{Os} = 1.40$, $^{186}\text{Os}/^{188}\text{Os} = 0.119880$; ultramafic rocks, 3 ppb Os, $^{187}\text{Os}/^{188}\text{Os} = 0.127$, $^{186}\text{Os}/^{188}\text{Os} = 0.119834$ (chondritic), black shales, 2 ppb Os, $^{187}\text{Os}/^{188}\text{Os} = 9.3$, $^{186}\text{Os}/^{188}\text{Os} = 0.119843$. A constraint on possible compositions of continental sources of Os to seawater is plotted using the average $^{187}\text{Os}/^{188}\text{Os}$ of riverine Os and the maximum allowable $^{186}\text{Os}/^{188}\text{Os}$ for this composition (circled cross, identical to point B, Fig. 2). Lines within the triangle delineate the relative proportions of a black shale and ultramafic end member (subhorizontal dashed lines) and relative proportions of the average UCC end member and a black-shale/ultramafic mixture (subvertical solid lines). (A) Physical mixtures of the three components. (B) Mixtures of the three components taking into account that black shales are weathered more efficiently than felsic rocks (details in text).

model mixing sensitivities. The Os parameters chosen for each of the end members are intended to test the influence of extreme compositions while retaining a conservative model. The model is not meant to accurately estimate actual mixing proportions.

Dissolved Os in rivers has an estimated average $^{187}\text{Os}/^{188}\text{Os}$ of 1.54 (Levasseur et al., 1999; horizontal dashed arrow, Fig. 2). Levasseur et al. (1999) assign a large uncertainty (20%) to this estimate, and a riverine estimate does not account for estuarine processes. With these caveats, for comparison this can be taken as a working estimate for the $^{187}\text{Os}/^{188}\text{Os}$ of the current continental source of Os to seawater. A $^{187}\text{Os}/^{188}\text{Os}$ of 1.54 requires that the $^{186}\text{Os}/^{188}\text{Os}$ of such a source be approximately 0.119844 or less (point B, Fig. 2). This composition is also plotted on Figure 3.

The isotopic consequences of physical mixing of the three components (with no differences in chemical weathering susceptibility) are examined in Figure 3A. This might correspond to a scenario in which sampling preferences arise strictly from systematic disparities in the geographic occurrences of these rock types, and although not a likely scenario, is a useful starting point for comparison. In this case, amending average UCC model compositions by adding 2% black shale and 3% ultramafic end members to 95% average UCC results in a mixture that satisfies the requirements for a continental end member imposed by the data (Fig. 3A). A relative ease of weathering is factored into the model in Figure 3B. Black shales may be 45 to 90 times more efficient at releasing Os to the hydrosphere as granitic rocks (Peucker-Ehrenbrink and Hannigan, 2000). The more conservative factor of 45 is applied to the black shales end member in our model (Fig. 3B). Taking this into consideration, the addition of only ~0.04% black shale and 1.36% ultramafic rocks to average UCC is required to explain the data (Fig. 3B). This means that a source with the composition of average UCC can make up to 97% of the continental end member and the $^{186}\text{Os}/^{188}\text{Os}$ of seawater would be only approximately 60 ppm enriched over chondrites and within error of our estimate for seawater.

For these calculations, we chose compositional variables to provide a rigorous test of the model. Accordingly, using less restrictive values require less additional black shale and ultramafic rock to drive the composition of seawater. The calculations are especially sensitive to the relative weathering efficiencies for each rock type, thus if black shales are more than 45 times as efficient at releasing Os than granitic rocks, then significantly less additional shale is required to explain the data. Similarly, the behavior of mafic and ultramafic rocks in the surface environment relative to average UCC will influence the effect that they have on the system.

Sediments and sedimentary rocks comprise approximately 75% of the exposed surface area of the earth. Of these sediments, approximately 50 to 70% are shales, and of shales, 5–10% have total organic carbon abundances of greater than 5%, enabling the calculation of an estimate of 2–5% for the total global outcrop area of black shales (Pettijohn, 1975; Blatt et al., 1980). This agrees with an independent estimate of 3% of land surface area being comprised of shales that are organic-rich or pyritic (Meybeck, 1987) and is in general agreement with calculations for Himalayan basins which indicate that black shales must comprise between 1 to 2% of outcrop area to explain the Os isotopic compositions and Re concentrations of rivers (Pierson-Wickmann et al., 2000; Dalai et al., 2002). The addition or subtraction of less than a tenth of a percent of a high $^{187}\text{Os}/^{188}\text{Os}$ black shale to or from weathered crust globally can have a profound effect on seawater $^{187}\text{Os}/^{188}\text{Os}$ (Fig. 3B), and

the implications suggested by the modeling are plausible in light of the areal availability of black shales.

Large ranges in Os isotopic composition are possible among and within river basins, often as a result of changing point sources (i.e., preferential sampling) on basin-wide scales. The total range of riverine compositions reported by Levasseur et al. (1999) is highly variable, with $^{187}\text{Os}/^{188}\text{Os}$ from 0.23 (Iceland) to 2.94 (Ganges). Levasseur et al. (1999) recorded seasonal changes in the Os concentration and $^{187}\text{Os}/^{188}\text{Os}$ of some rivers of up to 30% between high and low stages. Chesley et al. (2000) reported changes in the $^{187}\text{Os}/^{188}\text{Os}$ of paleosols over the last 15 Ma by up to a factor of two in both the Ganges ($^{187}\text{Os}/^{188}\text{Os} \sim 0.5$ to 1) and Indus River ($^{187}\text{Os}/^{188}\text{Os} \sim 1.6$ to 2.6) systems. In a study of Himalayan rivers, Sharma et al. (1999) concluded that the differences in $^{187}\text{Os}/^{188}\text{Os}$ of rivers draining radiogenic sources (e.g., $^{187}\text{Os}/^{188}\text{Os}$ of ~ 1.6 for the Ganges sampling black shales) and rivers draining sources with lower $^{187}\text{Os}/^{188}\text{Os}$ (e.g., $^{187}\text{Os}/^{188}\text{Os}$ of 1.1 to 1.2 for the Indus and Brahmaputra sampling ophiolites) are minor and testify to the tendency of large river basins to average changes and effectively buffer extreme compositions. Given the size of the Himalayan drainage system however, the fact that ranges of this magnitude exist at all is significant, and alludes to the ability of differential weathering to alter river chemistries globally and over long time periods. The ability of source regions with black shales and ultramafic rocks to heavily and persistently influence the Os isotopic composition of rivers which drain them are documented in studies of Himalayan rivers, the Baltic Sea, and rivers feeding Oneida Lake, NY (Pegram et al., 1994; Peucker-Ehrenbrink and Ravizza, 1996; Sharma et al., 1999; Dalai et al., 2002).

4.2. Possible Secular Variations in the $^{187}\text{Os}/^{188}\text{Os}$ of Seawater

If the flux of cosmic sources of Os is constant, and variations in the $^{187}\text{Os}/^{188}\text{Os}$ of marine Mn nodules reflect the evolution of seawater $^{187}\text{Os}/^{188}\text{Os}$, then the average age of each analyzed sample of Mn nodule can be estimated, and their $^{186}\text{Os}/^{188}\text{Os}$ ratios can be crudely related to the age of deposition. Two analyzed Mn nodules show evidence for the addition of ^{186}Os -enriched Os to the oceans in the past (Table 1, Fig. 1). One of three aliquants of sample VM21-D5 has a $^{187}\text{Os}/^{188}\text{Os}$ of 0.850, and a $^{186}\text{Os}/^{188}\text{Os}$ that is significantly enriched relative to chondrites by ~ 250 ppm. Similarly, one of two aliquants of sample VM15-SBT151 shows a minimum of 60 ppm enrichment of ^{186}Os with a corresponding $^{187}\text{Os}/^{188}\text{Os}$ of 0.967. The ^{186}Os -enriched aliquant of VM21-D5 has a $^{187}\text{Os}/^{188}\text{Os}$ consistent with an integrated model formation age of approximately 16 Ma whereas the enriched aliquant of VM15-SBT151 has an integrated model age of < 2 Ma. These enrichments may reflect times when the weathering of black shales and continental ultramafic rocks decreased relative to the weathering of more characteristic UCC with high long term Pt/Os. At present, it is premature to speculate much on these analyses, however. Further analyses of Mn nodules, including multiple replications of both high and low $^{186}\text{Os}/^{188}\text{Os}$ aliquants (as was done in this study for VM19-D11) will be necessary to begin to address this question.

4.3. Open Questions and Future Directions

It is apparent from the data available that the current continental source of Os to seawater is not identical to average UCC as it is presently characterized. Differential sampling of minor crustal components during weathering and denudation (e.g., black shales and ultramafic rocks) can have a significant impact on the isotopic composition of seawater. That black shales are capable of driving changes in seawater $^{187}\text{Os}/^{188}\text{Os}$ does not mean that they do drive those changes, however. The resolution of several issues will go far towards better understanding the mass balance of continental sources of Os to the world's oceans. Arguments presented here rely on a few assumptions that will either strengthen or weaken with additional data.

Additional careful measurements of Mn nodules, as was done for sample VM19-D11, will be important, as will a better characterization of the average $^{186}\text{Os}/^{188}\text{Os}$ of average UCC and of the range of $^{187}\text{Os}/^{188}\text{Os}$ and $^{186}\text{Os}/^{188}\text{Os}$ for black shales. The modeling in Figure 3A provides insight into not only how preferential sampling of continental crust by rivers can influence the composition of mixtures, but also into how sensitive measurements of average UCC are to similar preferential sampling by loess. We did not address the effects of chemical weathering on ultramafic rocks although the role that they play in the model is crucial. Ultramafic rocks are more susceptible to weathering than are felsic rocks (Meybeck, 1987), but it is not clear whether Os is easily mobilized from its host phases during weathering. A better understanding of the behavior of Os during weathering of ultramafic lithologies would be helpful.

A careful analysis of the global distribution of rock types and Os in the exposed continental crust is imperative for a complete understanding of the Os isotopic composition of modern seawater. For instance, relative to the size of drainage basins or continents, are black shales or ultramafic rocks (or other lithologies with remarkable Os compositions) generally distributed homogeneously, or are there patterns in their occurrence? Are they more common in some types of tectonic settings or on some continents than others? If the geographic distribution of black shales or ultramafic rocks is systematically heterogeneous, then it is not only possible, but probable that changes in global weathering and erosion patterns will result in changes in the Os isotopic composition of seawater over time.

5. CONCLUSIONS

Used in conjunction with the Re-Os system, the Pt-Os isotope system provides evidence that minor lithologies within upper continental crust can have a significant influence on the Os budget of modern seawater over time, particularly as those lithologies have high Os abundances and isotopic compositions that are very different from estimates for average UCC. The results of a conservative model suggest that rivers draining UCC, with the addition of less than 0.1% black shale, can discharge into the world's oceans dissolved Os that is barely suprachondritic with respect to the Pt-Os system, yet highly radiogenic with respect to the Re-Os system. The addition of Os from the weathering of ultramafic rocks can also provide an input that is not only chondritic with respect to $^{186}\text{Os}/^{188}\text{Os}$, but also to $^{187}\text{Os}/^{188}\text{Os}$. The interplay of these two sources pro-

vides a mechanism by which the $^{187}\text{Os}/^{188}\text{Os}$ of seawater can change as sources and weathering conditions change, yet $^{186}\text{Os}/^{188}\text{Os}$ changes imperceptibly.

Acknowledgments—The authors thank the Lamont-Doherty Earth Observatory for samples of marine Mn nodules, Cornell Field Station for samples of Oneida Lake ferro-manganese crusts, and J. Zhong and G. N. Hanson (SUNY Stony Brook) for the loess samples. Two anonymous reviewers and B. Peucker-Ehrenbrink are thanked for their careful reviews. This work was partially supported by NSF CSEDI grant EAR 9804909 and NSF grant OCE 116955, which are gratefully acknowledged.

Associate editor: E. M. Ripley

REFERENCES

- Blatt H., Middleton G., and Murray R. (1980) *Origin of Sedimentary Rocks*. Prentice-Hall.
- Blum J. D., Gazis C. A., Jacobsen A. D., and Chamberlain C. P. (1998) Carbonate versus silicate weathering in the Raikhot watershed within the high Himalayan Crystalline Series. *Geology* **26**, 411–414.
- Brandon A. D., Norman M. D., Walker R. J., and Morgan J. W. (1999) ^{186}Os - ^{187}Os systematics of Hawaiian picrites. *Earth Planet. Sci. Lett.* **172**, 25–42.
- Brandon A. D., Snow J. E., Walker R. J., Morgan J. W., and Mock T. D. (2000) ^{190}Pt - ^{186}Os and ^{187}Re - ^{187}Os systematics of abyssal peridotites. *Earth Planet. Sci. Lett.* **177**, 319–335.
- Burke W. H., Denison R. E., Hetherington E. A., Koepnick R. B., Nelson H. F., and Otto J. B. (1982) Variation of seawater $^{87}\text{Sr}/^{86}\text{Sr}$ throughout Phanerozoic time. *Geology* **10**, 516–519.
- Burton K. W., Bourdon B., Birck J.-L., Allègre C. J., and Hein J. R. (1999) Osmium isotope variations in the oceans recorded by Fe-Mn crust. *Earth Planet. Sci. Lett.* **171**, 185–197.
- Chesley J. T., Quade J., and Ruiz J. (2000) The Os and Sr isotopic record of Himalayan paleorivers: Himalayan tectonics and influence on ocean chemistry. *Earth Planet. Sci. Lett.* **179**, 115–124.
- Cohen A. S., Coe A. L., Bartlett J. M., and Hawkesworth C. J. (1999) Precise Re-Os ages of organic-rich mudrocks and the Os isotope composition of Jurassic seawater. *Earth Planet. Sci. Lett.* **167**, 159–173.
- Creaser R. A., Sannigrahi P., Chacko T., and Selby D. (2002) Further evaluation of the Re-Os geochronometer in organic-rich sedimentary rocks: A test of hydrocarbon maturation effects in the Exshaw Formation, Western Canada Sedimentary Basin. *Geochim. Cosmochim. Acta* **66**, 3441–3452.
- Dalai T., Singh S. K., Trivedi J. R., and Krishnaswami S. (2002) Dissolved rhenium in the Yamuna River System and the Ganga in the Himalaya: Role of black shale weathering on the budgets of Re, Os, and U in rivers and CO_2 in the atmosphere. *Geochim. Cosmochim. Acta* **66**, 29–43.
- DePaolo D. J. (1986) Detailed record of the Neogene Sr isotopic evolution of seawater from DSDP Site 590B. *Geology* **14**, 103–106.
- Derry L. A. and France-Lanord C. (1996) Neogene Himalayan weathering history and river $^{87}\text{Sr}/^{86}\text{Sr}$: Impact on the marine Sr record. *Earth Planet. Sci. Lett.* **142**, 59–74.
- Esser B. K. and Turekian K. K. (1988) Accretion rate of extraterrestrial particles determined from osmium isotope systematics of Pacific pelagic clay and manganese nodules. *Geochim. Cosmochim. Acta* **52**, 1383–1388.
- Esser B. K. and Turekian K. K. (1993) The osmium isotopic composition of the continental crust. *Geochim. Cosmochim. Acta* **57**, 3093–3104.
- Gao S., Lou T.-C., Zhang B.-R., Zhang H.-F., Han Y.-W., Zhao Z.-D., and Hu Y.-K. (1998) Chemical composition of the continental crust as revealed by studies in east China. *Geochim. Cosmochim. Acta* **62**, 1959–1975.
- Hoffman E., Naldrett A., Van Loon J., Hancock R., and Mason A. (1978) The determination of all the platinum group elements and gold in rocks and ore by neutron activation analysis after preconcentration by a nickel sulfide fire-assay technique of large samples. *Anal. Chim. Acta* **102**, 157–166.
- Horan M. F., Morgan J. W., Grauch R. I., Coveney R., Murowchick J., and Hulbert L. (1994) Rhenium and osmium isotopes in black shales and Ni-Mo-PGE-rich sulfide layers, Yukon Territory, Canada, and Hunan and Guizhou provinces China. *Geochim. Cosmochim. Acta* **58**, 257–265.
- Jaffe L. A., Peucker-Ehrenbrink B., and Petsch S. T. (2002) Mobility of rhenium, platinum group elements and organic carbon during black shale weathering. *Earth Planet. Sci. Lett.* **198**, 339–353.
- Levasseur S., Birck J.-L., and Allègre C. J. (1998) Direct measurement of femtomoles of osmium and the $^{187}\text{Os}/^{186}\text{Os}$ ratio in seawater. *Science* **282**, 272–274.
- Levasseur S., Birck J.-L., and Allègre C. J. (1999) The osmium riverine flux and the oceanic mass balance of osmium. *Earth Planet. Sci. Lett.* **174**, 7–23.
- Luck J.-M. and Turekian K. K. (1983) Osmium-187/osmium-186 in manganese nodules and the Cretaceous-Tertiary boundary. *Science* **222**, 613–615.
- Lyle M. (1982) Estimating growth rates of manganese nodules from chemical compositions: Implications for nodule formation processes. *Geochim. Cosmochim. Acta* **46**, 2301–2306.
- MacArthur J. M., Howarth R. J., and Bailey T. R. (2001) Strontium isotope stratigraphy: LOWESS version 3: Best fit to the marine Sr-isotope curve for 0–509 Ma and accompanying look-up table for deriving numerical age. *J. Geol.* **109**, 155–170.
- Meybeck M. (1987) Global chemical weathering of surficial rocks estimated from river dissolve loads. *Am. J. Sci.* **287**, 401–428.
- Miller R. G., O'Nions R. K., Hamilton P. J., and Welin E. (1986) Crustal residence ages of clastic sediments, orogeny and continental evolution. *Chem. Geol.* **57**, 87–99.
- Morgan J. W., Walker R. J., Horan M. F., Beary E. S., and Naldrett A. J. (2002) ^{190}Pt - ^{186}Os and ^{187}Re - ^{187}Os systematics of the Sudbury Igneous Complex, Ontario. *Geochim. Cosmochim. Acta* **66**, 273–290.
- Palmer M. R. and Edmond J. M. (1989) The strontium isotope budget of the modern ocean. *Earth Planet. Sci. Lett.* **92**, 11–26.
- Palmer M. R. and Turekian K. K. (1986) $^{187}\text{Os}/^{186}\text{Os}$ in marine manganese nodules and the constraints on the crustal geochemistries of rhenium and osmium. *Nature* **319**, 216–220.
- Palmer M. R., Falkner K. K., Turekian K. K., and Calvert S. E. (1988) Sources of osmium isotopes in manganese nodules. *Geochim. Cosmochim. Acta* **52**, 1197–1202.
- Pegram W. J., Krishnaswami S., Ravizza G. E., and Turekian K. K. (1992) The record of sea water $^{187}\text{Os}/^{186}\text{Os}$ variation through the Cenozoic. *Earth Planet. Sci. Lett.* **113**, 569–576.
- Pegram W., Esser B., Krishnaswami S., and Turekian K. K. (1994) The isotopic composition of leachable osmium from river sediments. *Earth Planet. Sci. Lett.* **128**, 591–599.
- Pettijohn F. J. (1975) *Sedimentary Rocks*. Harper & Row.
- Peucker-Ehrenbrink B., Ravizza G., and Hofmann A. (1995) The marine $^{187}\text{Os}/^{186}\text{Os}$ record of the past 80 million years. *Earth Planet. Sci. Lett.* **130**, 155–167.
- Peucker-Ehrenbrink B. and Ravizza G. (1996) Case study of continental run-off of Os: The Baltic Sea. *Geology* **24**, 327–330.
- Peucker-Ehrenbrink B. and Hannigan R. E. (2000) Effects of black shale weathering on the mobility of rhenium and platinum group elements. *Geology* **28**, 475–.
- Peucker-Ehrenbrink B. and Jahn B. (2001) Rhenium-osmium isotope systematics and platinum group element concentrations: Loess and the upper continental crust. *Geochem. Geophys. Geosyst.* **2**, GC000172.
- Pierson-Wickmann A.-C., Reisberg L., and France-Lanord C. (2000) The Os isotopic composition of Himalayan river bedloads and bedrocks: Importance of black shales. *Earth Planet. Sci. Lett.* **176**, 203–218.
- Quade J., Roe L., DeCelles P. G., and Ojha T. P. (1997) The Late Neogene $^{87}\text{Sr}/^{86}\text{Sr}$ record of lowland Himalayan rivers. *Science* **276**, 1828–1831.
- Ravizza G. (1993) Variations of the $^{187}\text{Os}/^{186}\text{Os}$ ratio of seawater over the past 28 million years as inferred from metalliferous carbonates. *Earth Planet. Sci. Lett.* **118**, 335–348.
- Ravizza G. and Esser B. K. (1993) A possible link between the seawater osmium isotope record and weathering of ancient sedimentary organic matter. *Chem. Geol.* **107**, 255–258.

- Ravizza G. and Pyle D. (1997) PGE and Os isotopic analysis of single sample aliquots with NiS fire assay preconcentration. *Chem. Geol.* **141**, 251–268.
- Ravizza G., Peucker-Ehrenbrink B., and Tuit C. B. (1998) Osmium isotopes as tracers of organic matter weathering. *Eos* **79**, F427.
- Raymo M. E. and Ruddiman W. F. (1992) Tectonic forcing of late Cenozoic climate. *Nature* **359**, 117–122.
- Reusch D. N., Ravizza G., Maasch K. A., and Wright J. D. (1998) Miocene seawater $^{187}\text{Os}/^{188}\text{Os}$ ratios inferred from metalliferous carbonates. *Earth Planet. Sci. Lett.* **160**, 163–178.
- Ripley E. M., Park Y.-R., Lambert D. D., and Frick L. R. (2001) Re-Os isotopic composition and PGE contents of Proterozoic carbonaceous argillites, Virginia Formation, Northeastern Minnesota. *Org. Geochem.* **32**, 857–866.
- Sharma M. and Wasserburg G. J. (1997) Osmium in the rivers. *Geochim. Cosmochim. Acta* **61**, 5411–5416.
- Sharma M., Papanastassiou D. A., and Wasserburg G. J. (1997) The concentration and isotopic composition of osmium in the oceans. *Geochim. Cosmochim. Acta* **61**, 3287–3299.
- Sharma M., Wasserburg G. J., Hofmann A. W., and Chakrapani G. J. (1999) Himalayan uplift and osmium isotopes in oceans and rivers. *Geochim. Cosmochim. Acta* **63**, 4005–4012.
- Shirey S. B. and Walker R. J. (1998) The Re-Os isotope system in cosmochemistry and high-temperature geochemistry. *Ann. Rev. Earth Planet. Sci.* **26**, 423–500.
- Singh S. K., Trivedi J. R., and Krishnaswami S. (1999) Re-Os systematics in black shales from the Lesser Himalaya: Their chronology and role in the $^{187}\text{Os}/^{188}\text{Os}$ evolution of seawater. *Geochim. Cosmochim. Acta* **63**, 2381–2392.
- Walker R. J., Morgan J. W., Naldrett A. J., Li C., and Fassett J. D. (1991) Re-Os isotope systematics of Ni-Cu sulfide ores, Sudbury Igneous Complex: Evidence for a major crustal component. *Earth Planet. Sci. Lett.* **105**, 416–429.
- Walker R. J., Morgan J. W., Smoliar M. I., Beary E., Czamanske G. K., and Horan M. F. (1997) Applications of the ^{190}Pt - ^{186}Os isotope system to geochemistry and cosmochemistry. *Geochim. Cosmochim. Acta* **61**, 4799–4808.
- Walker R. J., Hemming S. R., Becker H., and Hodgson M. (1999) Osmium-186 isotopic systematics of manganese nodules and marine sediments. *Ann. Goldschmidt Conf.* **9**, 315.
- Walker R. J., Prichard H. M., Ishiwatari A., and Pimentel M. (2002) The osmium isotopic composition of convecting upper mantle deduced from ophiolite chromites. *Geochim. Cosmochim. Acta* **66**, 329–345.
- Wedepohl K. H. (1995) The composition of the continental crust. *Geochim. Cosmochim. Acta* **59**, 1217–1232.
- Williams G. A. and Turekian K. K. (2002) Atmospheric supply of osmium to the oceans. *Geochim. Cosmochim. Acta* **66**, 3789–3791.
- Woodhouse O. B., Ravizza G., Kenison Falkner K., Staham P. J., and Peucker-Ehrenbrink B. (1999) Osmium in seawater: Vertical profiles of concentration and isotopic composition in the eastern Pacific Ocean. *Earth Planet. Sci. Lett.* **173**, 223–233.